ORIGINAL ARTICLE

Benefits of Brain Dual-Energy CT Imaging in Detecting Intracranial Hemorrhage in Non-Contrast Brain CT Scans

Pipat Chiewvit, MD[1], Siriwan Piyapittayanan, MD[1], Chanon Ngamsombat, MD[1], Tipa Chakorn, MD[2]

[1] Division of Diagnostic Radiology, Department of Radiology, Faculty of Medicine Siriraj Hospital, Mahidol University, Bangkok, Thailand; [2] Department of Emergency Medicine, Faculty of Medicine Siriraj Hospital, Mahidol University, Bangkok, Thailand

Background: Non-contrast brain computed tomography (CT) scans are the gold standard for diagnosing intracranial hemorrhage (ICH). However, the scans have evaluation limitations, especially in cases of interfering bony artifacts, and overlapping hypoattenuating calcifications and hemorrhages. Material decomposition dual-energy CT (DECT) can separate materials based on atomic numbers.

Objective: To compare the diagnostic accuracy, sensitivity, and specificity of material decomposition non-contrast DECT of the brain with conventional 120 kVp-single energy CT (SECT) imaging for ICH diagnosis.

Materials and Methods: The present study was a retrospective study conducted at a single center. Three neuroradiologists separately and blindly reviewed the postprocessing images of 111 patients with 215 lesions. DECT acquisitions generated the images. They were in the form of 1) SECT images, 2) blood-subtracted calcium, non-overlay images as "blood (calcium) non-overlay" images, 3) blood-subtracted calcium, overlay images with rainbow and grayscale color-coding as "blood (calcium) overlay" images, and 4) combined SECT and blood-subtracted calcium, overlay images as "combined SECT + blood (calcium) overlay" images.

Results: Compared with the SECT images, the blood (calcium) overlay images had better accuracy, at 99.6%, sensitivity at 99.5%, and specificity at 100% for ICH diagnosis. The blood (calcium) overlay images also provided better observer confidence, a 94.06% certain diagnosis, than the SECT images ($p<0.05$). The blood (calcium) overlay images and combined images had very good interrater reliability, whereas the reliability of the SECT images was poor.

Conclusion: Material decomposition DECT, as either blood (calcium) overlay images or combined SECT + blood (calcium) overlay images, has a high ICH diagnostic ability in non-contrast brain CT imaging.

Keywords: Dual energy CT; Noncontrast CT brain; Intracranial hemorrhage; ICH

Received 7 December 2023 | Revised 1 July 2024 | Accepted 26 July 2024

J Med Assoc Thai 2024;107(9):690-700

Website: http://www.jmatonline.com

Head injury is a severe problem in all countries due to its high morbidity and mortality. The incidence of head injury varies depending on the terminology used and the data collection method. In 2013, traumatic brain injuries were diagnosed in 2.8 million of the 26 million injury-related emergency department visits, hospitalizations, and deaths that occurred in the United States[1]. In Thailand, 42.7% of severe injury cases related to motorcycle accidents had head injuries, and the corresponding figure in cases of death was 70.8%[2].

Correspondence to:

Chiewvit P.

Division of Diagnostic Radiology, Department of Radiology, Faculty of Medicine Siriraj Hospital, Mahidol University, Bangkok 10700, Thailand.

Phone: +66-86-3604757

Email: pipat.chi@mahidol.ac.th

How to cite this article:

Chiewvit P, Piyapittayanan S, Ngamsombat C, Chakorn T. Benefits of Brain Dual-Energy CT Imaging in Detecting Intracranial Hemorrhage in Non-Contrast Brain CT Scans. J Med Assoc Thai 2024;107:690-700.
DOI: 10.35755/jmedassocthai.2024.9.690-700-576

Computed tomography (CT) interpretation of intracranial hemorrhage (ICH) is based on attenuation in biological tissues. The attenuation of the tissue is associated with its atomic number and physical density. Magnetic resonance imaging (MRI) can provide more accurate information as compared to CT about the stage of the hematoma by identifying the sequential patterns of transformation of hemoglobin within the hematoma[3]. However, MRI has limited availability and requires a long scan time. Thus, non-contrast CT remains the diagnostic test of choice in acute intracerebral hemorrhage because of its sensitivity to acute hemorrhage, short scan time, low cost, widespread availability, and the technical ease of obtaining a scan even with acutely ill patients[4]. Nevertheless, CT scans still have limitations in evaluating small lesions and lesions close to the skull base and posterior fossa. Such lesions may interfere with bony artifacts and can easily be misdiagnosed[5].

Hyperattenuated materials in non-contrast CT scans can arise from two common causes: hemorrhage

and calcium. The other less common causes are high proteinaceous substances and hypercellular tissue. In non-contrast CT images, acute hemorrhage has an attenuation range of 60 to 100 Hounsfield units (HU)[6], whereas calcified lesions have an attenuation greater than 100 HU. However, calcification can also have varying attenuations. These can be less than 100 HU, depending on the amount of calcium deposit. Therefore, there is an overlap between the attenuation values of low attenuation intracranial calcification, or less than 100 HU, and hemorrhage. Furthermore, they also show the blooming effect of the susceptibility weighted imaging (SWI) sequence. These shortcomings may lead to misinterpretations[7] and inappropriate management.

A dual-energy CT (DECT) scan is a new CT scanning technology that generates material-specific images based on a particular material's atomic number and unique mass attenuation coefficient at different X-ray energies. Material-specific images provide qualitative and quantitative information on tissue composition[8]. Moreover, DECT imaging is not associated with increased radiation dose levels[9]. Therefore, DECT scans are used for virtual monochromatic images, artifact suppression images, and material decomposition images. According to brain tissue, blood, and calcium/bone have different atomic numbers, modified from Yang et al[10]. The effective atomic number of blood is 7.59. It is different from that of calcium, which is 20.0. Consequently, DECT may provide improved diagnostic accuracy, sensitivity, and specificity in detecting ICHs in non-contrast DECT of the brain. The purpose of study was to determine the diagnostic accuracy, sensitivity, and specificity of non-contrast DECT of the brain in diagnosing any ICH compared with conventional 120 kVp-single energy CT (SECT) imaging. The secondary aims to collect the radiation dose and estimate the total scan time of non-contrast DECT imaging.

Materials and Methods

This retrospective study drew upon the picture archiving and communication system (PACS). After approval by the Institutional Ethics Committee, a review was made of all consecutive, non-contrast, DECT examinations of the brain performed at Siriraj Hospital between May 1, 2019, and January 31, 2020.

Ethical approval

The Siriraj Institutional Review Board (SIRB) approved the protocol of the present study. The SIRB protocol number of the study was 194/2563 (IRB1). Certify that the study was performed in accordance with the ethical standards as laid down in the 1964 Declaration of Helsinki and its later amendments or comparable ethical standards.

Study participants

Inclusion criteria:

The inclusion criteria were as follows:

- Patients who underwent non-contrast DECT of the brain at Siriraj Hospital between May 1, 2019, and January 31, 2020.
- Older than 18 years old.
- Confirmed diagnosis noted by clinical information in at least one of the following types of information, such as the outpatient department (OPD) card records, operative findings, or records related to a follow-up CT or MRI of the brain performed for any reason within one month after the first non-contrast DECT imaging.
- In the "negative group", patients who were approved for discharge by a clinician with "clinically negative for ICH" noted in the OPD card records. If there was a follow-up appointment, the patient did not have abnormal neurological symptoms that may have led to suspicion of ICH, such as nausea, vomiting, headache, or an abnormal neurological examination.

Exclusion criteria:

The exclusion criteria were as follows:

- Patients who did not undergo a non-contrast DECT scan of the brain at Siriraj Hospital.
- Patients who did not have a clinically confirmed diagnosis, either through CT or MRI of the brain performed within one month or via intraoperative findings.
- The postprocessing image from the DECT scan was of poor quality, or the related data file was incomplete.
- Patients who underwent an intracranial operation less than one year before the DECT was performed.

Image acquisition and postprocessing

The non-contrast DECT of the brain was performed at the authors' institution with a 256-slice, single-source, tube voltage switching, DECT scanner (Revolution CT scanner; GE Healthcare, Chicago, IL, USA) with a helical scan. The tube voltage was switched between 80 and 140 kV, while the tube current modulation was fixed at approximately 315 mA. Primary imaging reconstruction was performed at 65 keV.

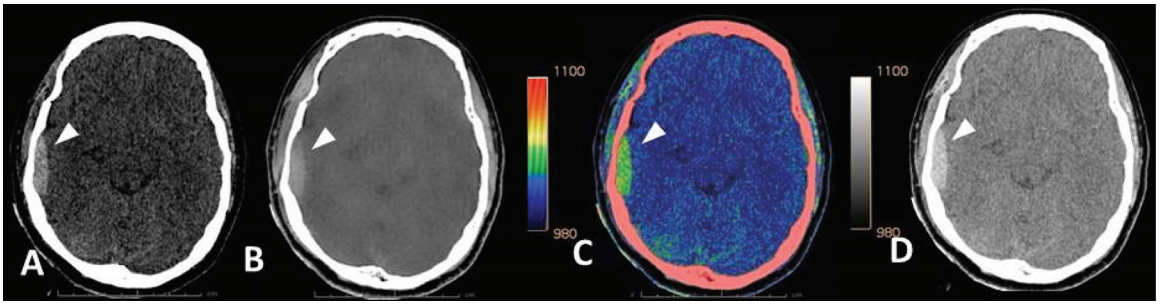

Figure 1. Four sets of images were separately interpreted by three neuroradiologists that were blinded patients' clinical context. Each set of images were reviewed separately at least two weeks apart from the prior set. The first test set is SECT images (A) showing epidural hemorrhage at right temporal lobe. The second test set is blood (calcium) images (B) showed lens-shaped hyperattenuation. The third test set are blood (calcium) overlay images in rainbow color coding (C) and greyscale color coding (D). The last test set are co-interpretation of SECT (A) and blood (calcium) image (B).

The retrospective postprocessing reconstruction images were obtained with material decomposition algorithm at 65 to 75 keV to maximize imaging quality, according to Pomerantz 2012[11]. This involved the axial view, a 2 mm-slice thickness without interval gap, a 50 to 104 window width, and a 1,000 to 1,040 window level. There were four data sets of images, 1) SECT images, 2) blood-subtracted calcium, non-overlay images as "blood (calcium) non-overlay" images, 3) blood-subtracted calcium, overlay images with rainbow and grayscale color-coding as "blood (calcium) overlay" images, and 4) combined SECT images and blood-subtracted calcium, overlay images as "combined SECT + blood (calcium) overlay" images.

Data analysis

Demographic data:

The demographic data of the enrolled patients were reviewed by one radiologist independently from the neuroradiologist readers. The following demographic data were obtained from electronic OPD card records:

- Patient age
- Patient gender: male/female
- Cause of injury: falling, traffic accident, or other
- Glasgow Coma Scale (GCS) score
- Final clinical diagnosis of ICH: type, stage, location
- Clinical management: discharged, referred out, admitted for conservative treatment or for observation of their neurological signs and symptoms, surgery, death, admitted due to a cause other than ICH, discharged against advice
- Confirmation of diagnosis: follow-up CT imaging of the brain within one month with follow-up CT scanning within 48 hours or more than 48 hours, follow-up MRI of the brain within one month, follow-up clinical context, surgery with a positive operative finding of ICH, and death with/without an autopsy
- Radiation dose: CT dose index volume ($CTDI_{vol}$; mGy), total dose-length product (mGy-cm)
- Scan time (msec)

Image analysis:

Postprocessing of the DECT images of the enrolled patients was performed by one specialist in the research team. It was conducted independently from the neuroradiologist readers. After that, the postprocessing images were obtained as four sets of images (Figure 1):

- SECT images
- Blood-subtracted calcium, non-overlay images as blood (calcium) non-overlay images
- Blood-subtracted calcium, overlay images with rainbow and grayscale color-coding as blood (calcium) overlay images
- SECT co-interpreted with blood (calcium), overlay images as combined SECT + blood (calcium) overlay images.

Lesions that still appeared hyperattenuating in blood (calcium) non-overlay images were classified as hemorrhagic lesions. However, lesions that showed isoattenuation or hypoattenuation in blood (calcium) non-overlay images were classified as non-hemorrhagic tissues. In blood (calcium) overlay images, lesions highlighted in yellow and green with rainbow color-coding or appearing hyperattenuated with grayscale color-coding were classified as hemorrhagic lesions. Lesions with any other color with rainbow color-coding or lesions with isoattenuation or hypoattenuation as grey and black with the grayscale color-coding, were classified as non-hemorrhagic (Figure 1, Table 1).

Table 1. Criteria used for classification of lesion

Type of lesion	Appearance on each image set			
	SECT	Blood (calcium)	Blood (calcium) overlay	
			Rainbow color code	Greyscale color code
Hemorrhagic lesion	hyperattenuating	hyperattenuating	yellow-green color	hyperattenuating
Non-hemorrhagic lesion	Iso-/hypoattenuating	Iso-/hypoattenuating	Any color (blue/orange/red color)	Iso- or hypoattenuating (grey-black color)

SECT=single energy computed tomography

All images were interpreted independently by three neuroradiologists, with more than eight years of experience, who were blinded to the patients' clinical contexts, any prior or follow-up imaging, and other observers' reports. Multifocal ICHs of the same type in the same area were recorded as one lesion to avoid overcounting non-independent lesions, such as multifocal hemorrhages. Multifocal ICHs of different types or from different areas in the same patient were recorded as separate lesions.

Each set of images was reviewed separately at least two weeks after the initial assessment, blinding to the prior report. Each observer gave each lesion a confidential reporting score. The scores were 2 for a "certain diagnosis", 1 for a "probable diagnosis", and 0 for a "doubtful diagnosis".

The data were recorded, and the lesion subgroups were categorized by a radiology resident as follows:

ICH:

1. Positive subgroup

Patients in this subgroup were classified in this manner:

- Type of ICH (5): epidural hemorrhage (EDH), intraparenchymal hemorrhage (IPH), intraventricular hemorrhage (IVH), subarachnoid hemorrhage (SAH), and subdural hemorrhage (SDH)
- Stage of ICH (3): acute, subacute, and chronic
- Size: The sizes of measurable lesions, such as EDH, IPH, and SDH types, were recorded at the maximal thickness (cm) for EDH and SDH and the maximal dimension (cm) for IPH. The lesions were classed as small for less than 1 cm or large for more than 1 cm.
- Location:
  - By area: the falx-tentorium-parasagittal area, cerebral hemisphere, base/inferior brain adjacent to the skull base, posterior fossa, intraventricular space, and other subarachnoid space not along sulci and gyri of the cerebral hemisphere
  - By lobe: frontal, parietal, temporal, occipital, brainstem, and cerebellum
  - By side: left, right, and bilateral
  - By IPH location: deep and lobar

2. Negative subgroup

The final imaging diagnosis was reviewed from the concordant diagnosis between two readers. If there was an asynchronous diagnosis, the third reader reviewed, and a consensus was reached to obtain the final diagnosis. The reference standard of negative or positive hemorrhage was established by consensus diagnosis. The diagnosis was correlated with commonly used and relevant prior or follow-up CT or MRI imaging and the available clinical information. Intraoperative findings were also used to determine the reference standard when available.

Furthermore, in the positive-ICH group, when a subsequent CT scan of the brain within 48 hours after the DECT imaging was recorded, the initial and follow-up lesion size, and initial and follow-up lesion HU in non-contrast imaging was also recorded.

Statistical analysis

Categorical independent variables such as gender, cause of injury, clinical management, and confirmation of diagnosis, are presented as numbers or percentages. Continuous data such as age, radiation dose, and scan time were reported as the mean ± standard deviation (SD). The GCS scores were analyzed as the median (minimum, maximum) as an appropriated distribution. The associations for univariate analysis and the categorical independent variables of the positive and negative subgroups as age, gender, cause of injury, GCS score, clinical management, and confirmation of diagnosis, were compared.

The diagnostic performance of the SECT images, blood (calcium) non-overlay images, blood (calcium) overlay images, and combined SECT + blood (calcium) overlay images was analyzed by accuracy, sensitivity, and specificity with 95% confidence interval (CI). Subgroup analyses, such as type, stage, size, and location, were performed by the chi-square test. The significance of continuous variables as two-independent samples was assessed with independent t-tests or Mann-Whitney U tests. Interrater reliability was carried out by Cohen's kappa and 95% CIs. A

Table 2. Demographic data shows patient and disease

Characteristics	Positive group (n=58)	Negative group (n=53)	p-value
Age (years); mean±SD	49.40±22.50	64.74±20.22	<0.001
Sex; n (%)			0.081
Male	39 (67.2)	27 (50.9)	
Female	19 (32.8)	26 (49.1)	
Cause of injury; n (%)			<0.001
Falling	20 (34.5)	38 (71.7)	
Traffic	31 (53.4)	7 (13.2)	
Other	7 (12.1)	8 (15.1)	
Minimum GCS score	2T	6	<0.001
Clinical management; n (%)			<0.001
Discharged	2 (3.4)	29 (54.7)	
Referred out	8 (13.8)	1 (1.9)	
Admitted for conservative management	33 (56.9)	2 (3.8)	
Admitted due to other cause	5 (8.6)	21 (39.6)	
Surgery	6 (10.3)	0 (0.0)	
Against advised	1 (1.7)	0 (0.0)	
Death	3 (5.2)	0 (0.0)	
Confirmation of diagnosis; n (%)			<0.001
F/U brain CT scan ≤1 month	24 (41.4)	7 (13.2)	
F/U brain CT scan ≤48 hours	17 (29.3)	4 (7.5)	
F/U brain CT scan >48 hours to 1 month	7 (12.1)	3 (5.7)	
F/U brain MRI ≤1 month	2 (3.4)	1 (1.9)	
F/U clinical context	24 (41.4)	45 (84.9)	
Surgery with positive ICH	6 (10.3)	0 (0.0)	
Death with/without autopsy	2 (3.4)	0 (0.0)	

GCS=Glasgow Coma Scale; F/U=follow-up; CT=computed tomography; MRI=magnetic resonance imaging; ICH=intracranial hemorrhage; SD=standard deviation
2T=E1M1VT (E=eye, M=motor, V=verbal)

probability (p) value less than 0.05 was considered statistically significant.

Results

The authors' retrospective review of the data stored in the hospital's PACS found that 841 non-contrast DECT studies of the brain were performed at the authors' institution between May 1, 2019 and January 31, 2020. The authors excluded 730 studies as they failed to meet the inclusion criteria. Of those, 689 had incomplete PACS data files, 38 did not have neurological signs or symptoms noted in their electronic OPD records, one involved a recent intracranial operation, and two had more than seven intracranial hemorrhagic foci. Thus, 111 studies with 251 lesions were reviewed with 58 positive studies with 198 lesions and 53 negative studies with 53 lesions.

Demographic data

The present study enrolled 111 patients that included 59.5% males and 40.5% females. The mean age of positive-ICH patients was 49.40±22.50 years, which was significantly lower than that of negative-ICH patients at 64.74±20.22 years. The minimum GCS score was 2T for positive-ICH patients and 6 for negative-ICH patients (Table 2). The major cause of injuries was falling 52.3%. It was followed by traffic accidents for 34.2% and other causes for 13.5%, such as body assault and acute alteration of consciousness with suspected ICH.

Most positive-ICH patients (56.9%) were admitted for observation of their neurological signs and symptoms, follow-up brain CT imaging in 41.4%, or follow-up for other clinical reasons in 41.4%. Seventeen positive-ICH patients (29.3%) were followed up with a CT scan of the brain within 48 hours. Conversely, most negative-ICH patients (54.7%) were discharged from the OPD and 84.9% had a follow-up session (Table 2).

Diagnostic performance for ICH

The present study revealed that SECT images

Table 3. Diagnostic performance of the images set in diagnosis of ICHs, evaluated per lesion (n=251 lesions)

Test set	Accuracy (%) (95% CI)	Sensitivity (%) (95% CI)	Specificity (%) (95% CI)
SECT	79.7 (74.2 to 84.5)	76.8 (71.1 to 81.9)	90.6 (86.3 to 93.9)
Blood (calcium)	61.0 (54.7 to 67.1)	56.6 (50.2 to 62.8)	77.4 (71.7 to 82.4)
Blood (calcium) overlay	99.6 (97.8 to 100)	99.5 (97.6 to 100)	100 (98.5 to 100)
SECT + Blood (calcium)	92.8 (88.9 to 95.7)	90.9 (86.6 to 94.2)	100 (98.5 to 100)

SECT=single energy computed tomography; CI=confidence interval

Table 4. Diagnostic performance of the images set in diagnosis of ICHs, evaluated per lesion: subgroup analysis of the positive lesions (n=198 lesions) via types of ICHs

Test set	Type of ICH (n=198); n (%)					p-value
	IPH (n=29)	SDH (n=93)	EDH (n=17)	SAH (n=50)	IVH (n=9)	
SECT	25 (86.2)	67 (72)	15 (88.2)	37 (74.0)	8 (88.9)	0.306
Blood (calcium)	18 (62.1)	54 (58.1)	15 (88.2)	18 (36.0)	7 (77.8)	0.001*
Blood (calcium) overlay	29 (100)	93 (100)	17 (100)	49 (98.0)	9 (100)	0.562
SECT + Blood (calcium)	26 (89.7)	88 (94.6)	17 (100)	41 (82.0)	8 (88.9)	0.086

SECT=single energy computed tomography; ICH=intracranial hemorrhage; IPH=intraparenchymal hemorrhage; SDH=subdural hemorrhage; EDH=epidural hemorrhage; SAH=subarachnoid hemorrhage; IVH=intraventricular hemorrhage

* Statistical significance

Table 5. Diagnostic performance of the images set in diagnosis of ICHs, evaluated per lesion: subgroup analysis of the positive lesions (n=198 lesions) via stages of ICHs

Test set	Stage of ICH (n=198); n (%)			p-value
	Acute (n=191)	Subacute (n=5)	Chronic (n=2)	
SECT	145 (75.9)	5 (100)	2 (100)	0.334
Blood (calcium)	108 (56.5)	2 (40.0)	2 (100)	0.351
Blood (calcium) overlay	190 (99.5)	5 (100)	2 (100)	0.982
SECT + Blood (calcium)	174 (91.1)	4 (80.0)	2 (100)	0.629

SECT=single energy computed tomography; ICH=intracranial hemorrhage

had a 79% diagnostic accuracy, 76.8% sensitivity, and 90.6% specificity (Table 3). SECT images were equivalent to the conventional single-energy CT scans commonly used as the gold standard for diagnosing ICH.

The blood (calcium) overlay images had the highest diagnostic accuracy at 99.6%, highest sensitivity at 99.5%, and highest specificity at 100%. All values were significantly higher than those of SECT images ($p<0.0001$).

In contrast, the blood (calcium) non-overlay images had the lowest diagnostic accuracy at 61.0%, lowest sensitivity at 56.6%, and lowest specificity at 77.4%. These values were significantly lower than those of SECT images ($p<0.0001$).

However, co-interpretation of the combined SECT + blood (calcium) overlay images increased diagnostic accuracy to 92.8%, sensitivity to 90.9%, and specificity to 100% ($p<0.0001$).

Subgroup analysis of the 198 positive lesions for the five ICH types, EDH, IPH, IVH, SAH, and SDH, revealed that blood (calcium) overlay images had the highest diagnostic accuracy for all types (Figure 2-3, Table 4).

The sizes of the 139 measurable lesions in EDH, IPH, and SDH, found by the present study were measured in the axial view and at the maximal dimension. In the case of EDH, the mean size was 2.55±4.15 cm. The thinnest EDH was 0.46 cm and was detected in all image sets (Table 5). There were no statistically significant differences between the image sets ($p=1.0000$).

The mean IPH size was 2.09±1.66 cm. The thinnest IPHs detected in the SECT, blood (calcium) non-overlay, blood (calcium) overlay, and combined SECT + blood (calcium) overlay images were 0.39, 0.39, 0.27, and 0.27-cm thick, respectively (Table 5). No statistically significant differences were found between each set of images ($p=0.7841$).

As for SDH, the mean size was 0.44±0.35 cm.

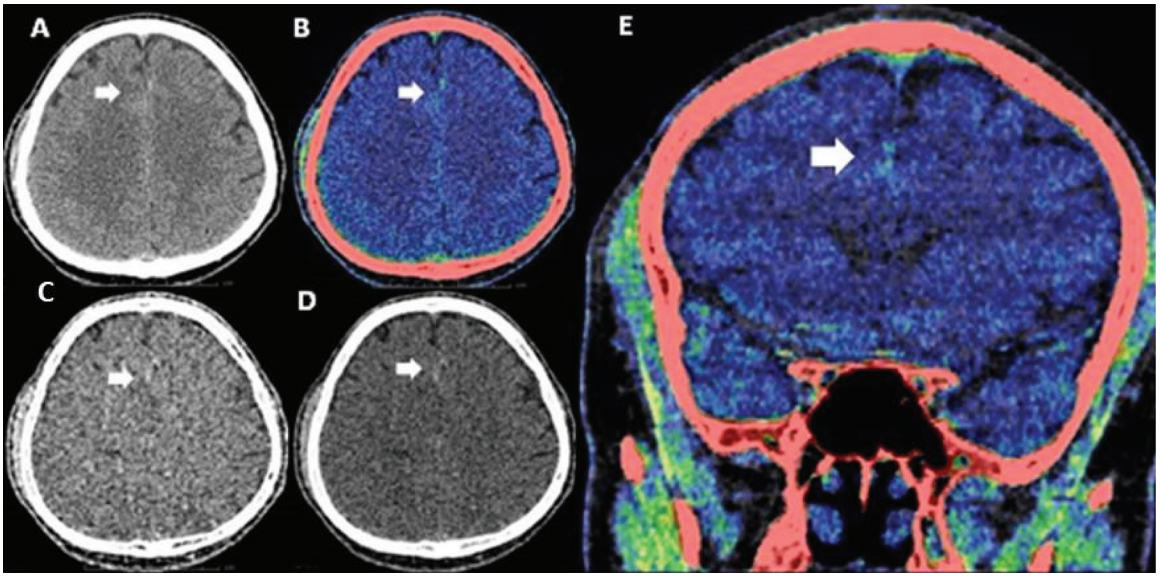

Figure 2. Showed faint SAH at parasagittal area (arrow) which was seen as faint hyper-attenuation on (A) SECT images, (B) blood (calcium) images still showed hyper-attenuation, and seen as green color on blood(calcium) overlay images (C) and hyper-attenuation on greyscale overlay images (D). Sagittal blood(calcium) overlay images with rainbow color coding (E) was still seen patchy green-color lesion at parasagittal area.

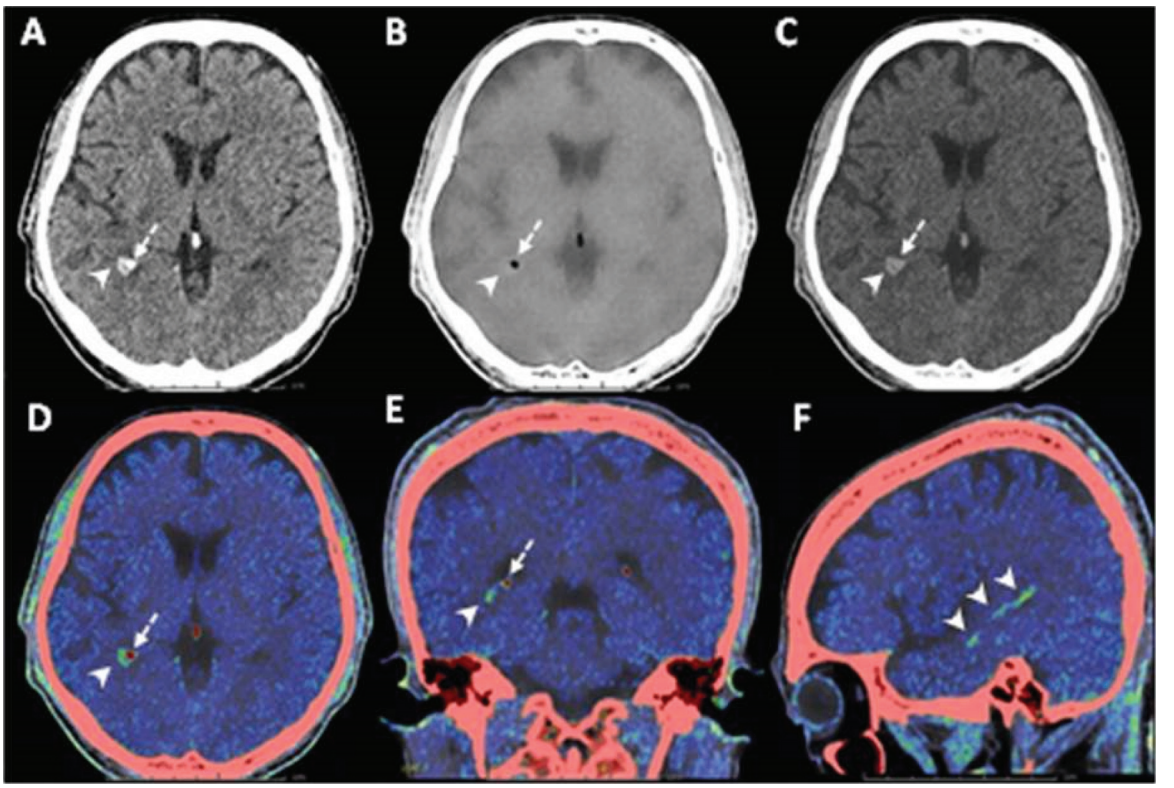

Figure 3. Showed small IVH in occipital and temporal horn of right lateral ventricle (big arrow head) seen as bright as the adjacent choroid plexus calcification (dash arrow) on SECT images (A). When subtraction calcium on blood(calcium) image (B), blood(calcium) overlay in greyscale color coding (C), it was clearly visualized as hyperattenuating lesion and showed green color on blood(calcium) overlay in rainbow color coding. (D, E, F), while the calcification (dash arrow) showed black color on blood(calcium) images, grey color on overlay images with greyscale color coding and red color on overlay images with rainbow color coding.

Table 6. Maximum and minimum size of the measurable ICHs, evaluated per lesion: subgroup analysis of the positive lesions (n=139 lesions) via type of the measurable ICHs

Image set	IPH (cm) (n=29)		SDH (cm) (n=93)		EDH (cm) (n=17)	
	Minimum	Maximum	Minimum	Maximum	Minimum	Maximum
Overall	0.27	6.03	0.12	2.66	0.46	18.10
SECT	0.39	6.03	0.14	2.66	0.46	18.10
Blood (calcium)	0.39	6.03	0.17	2.66	0.46	18.10
Blood (calcium) overlay	0.27	6.03	0.12	2.66	0.46	18.10
SECT + Blood (calcium)	0.27	6.03	0.12	2.66	0.46	18.10

SECT=single energy computed tomography; IPH=intraparenchymal hemorrhage; SDH=subdural hemorrhage; EDH=epidural hemorrhage

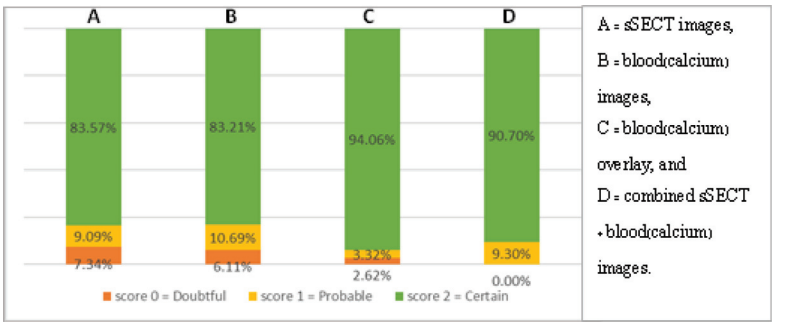

Figure 4. Showed percent of confident scores in diagnosis of ICHs among the four images series.

The thinnest SDH lesion was 0.12-cm thick and located along the falx cerebri. It could be detected only in blood (calcium) overlay images and the combined SECT + blood (calcium) overlay images. The thinnest SDH lesion visualized in SECT images was 0.14-cm thick. It was along falx cerebri. Blood (calcium) non-overlay imaging detected an SDH lesion as small as 0.17-cm thick in the left frontal area (Table 6). However, there were no statistically significant differences between each set of images (p=0.3313 to 0.6972).

Diagnoses confidence levels

The observers had the highest confidence in their ICH diagnosis when using blood (calcium) overlay images as 94.1% of diagnoses were rated "certain diagnosis". This confidence level was statistically significantly higher than the corresponding proportions for combined SECT and blood (calcium) overlay images ($p<0.05$) (Figure 4). This related to the fact that image quality of the acute hemorrhage derived from blood (calcium) grey scale image did not have the sharpness. Therefore, when it is used together with SECT, it may sometime lead to borderline interpretation. Whereas blood (calcium) color images can provide sharply delineated for differentiation material decomposition. However, there was no statistically significant difference from combined SECT + blood (calcium) overlay images. The authors may suggest using SECT as a routine first glance and then blood (calcium) color image to interpret acute ICH by DECT.

Interrater reliability

The interrater reliability was assessed for each image type. The ICH diagnosis was lowest when using SECT images (Cohen's kappa=0.38), which indicated poor agreement. Using blood (calcium) non-overlay and blood (calcium) overlay images improved interrater reliability to good agreement (Cohen's kappa=0.67 and 0.63, respectively).

Quality of DECT imaging assessments

The mean $CTDI_{vol}$ per study was 53.64±4.59 mGy, and the mean total dose-length product was 1,103.30±188.05 mGy-cm, which was equivalent to an effective dose of 2.32±0.39 mSv. The mean DECT scan duration was 53.92±19.16 seconds.

Discussion

Head injury is a severe problem in most countries and causes high morbidity and mortality. Non-contrast CT imaging is the gold standard for ICH diagnosis. However, it has limitations with the

evaluation of small lesions and with those located close to the skull base and the posterior fossa, where bony artifacts can cause interference[5]. The common hyperattenuating materials in non-contrast CT scans are hemorrhage and calcium. However, there is overlap attenuation between hemorrhage and low attenuation calcification. Nevertheless, hemorrhage, or blood, and calcium have individual atomic numbers that can be used to differentiate them in material decomposition DECT imaging. This distinction is advantageous because hemorrhage and calcification require different management approaches.

The present study enrolled 111 patients without different gender proportions between the positive- and negative-ICH groups. The mean age of the positive-ICH patients was significantly lower than that of the negative-ICH patients. The common cause of injury was a traffic accident. Such injuries are high energy and commonly occur in young, active-lifestyle patients. Additionally, the minimum GCS score of the positive-ICH group was lower than that of the negative-ICH group. This difference implies greater injury severity among the patients in the positive-ICH group. However, most of the positive-ICH patients were admitted for observation of their neurological signs and symptoms with a follow-up brain CT scan or some other clinical reason. Conversely, most negative-ICH patients had a higher minimum GCS score, and they may have been discharged without a follow-up appointment, given that they had less severe symptoms.

The results of the present study support the advantages of DECT scans in differentiating calcium from hemorrhage in phantom models[9,12] and human models[13,14], given its improved diagnosis of ICH in non-contrast CT images of the brain. However, only blood (calcium) overlay images and the combined SECT + blood (calcium) overlay images increased diagnostic accuracy, sensitivity, and specificity compared with SECT images alone, which did not depend on ICH type, stage, size, or location. The blood (calcium) overlay images also increased the observers' confidence levels and improved interrater reliability. Thus, material decomposition DECT can determine whether hyperattenuating lesions contain blood and minimize reader-related subjectivity, which is signified by the good interrater reliability. Moreover, the distinctive color of blood, especially in blood (calcium) overlay images, is easily detected by both neuroradiologists and non-radiologists. This attribute facilitates quick detection and decision-making about further management. The advantages of material decomposition DECT in discriminating between blood and calcium, correlating with clinical context, facilitate a decrease in unnecessary admissions and a reduction in the costs of hospitalizing negative-ICH patients.

On the other hand, the present study found that the blood (calcium) non-overlay images alone had inferior diagnostic accuracy, sensitivity, and specificity to SECT images. This finding could result from the poor image quality of blood (calcium) non-overlay images and the difficulty in discriminating the attenuation of the images. Nevertheless, the blood (calcium) non-overlay images improved interrater reliability. This increase resulted from their diagnostic ability being higher for large ICHs than small ICHs, which meant that every reader could easily detect large ICHs in the images. Thus, the authors do not recommend using blood (calcium) non-overlay images alone. They should be co-interpreted with SECT images.

The SECT images had the poorest diagnostic ability and the lowest interrater reliability, which would better detect large ICHs than small ones, and it was prone to subjective interpretation. Despite that, the SECT images still had the highest quality image due to their good grey-white differentiation.

The mean $CTDI_{vol}$ and effective radiation doses of DECT in the present study were equal to the radiation dose of SECT from a prior study[15-17]. The mean duration of the DECT scan per case was under a minute, which could be beneficial in an emergency setting. However, the postprocessing of images was slightly longer for DECT than for SECT.

Limitations exist in the present study. First, this was a retrospective design, and samples were unavailable for analysis due to incomplete data in postprocessing image files. Second, MRI studies of the brain were not performed to confirm the diagnoses in all cases due to resource limitations. Given that, the reference standards of the present study were based on consensus diagnoses correlated with commonly used relevant prior or follow-up CT or MRI imaging and clinical information. Third, the material decomposition DECT needs source data to process images. The data occupied a large data volume in a PACS, and the system needs to be stable for timely processing. Last, the present study's postprocessing images of overlay DECT could only be exported as screen-capture, which meant that multiplanar reconstruction could not be performed. Consequently, the observers had to interpret images only in the axial plane, which resulted in the misdiagnosis of lesions.

Conclusion

Material decomposition DECT scans, especially blood (calcium) overlay images, increased the diagnostic accuracy, sensitivity, and specificity for ICHs in non-contrast brain CT scans and increased the observer confidence level and interrater reliability. Material decomposition DECT is helpful, especially with uncertain hyperattenuating foci that are unclear in conventional CT images alone. The distinctive color of blood in blood (calcium) overlay images can be easily detected even by non-radiologists. This attribute might facilitate quick decision-making about further management in emergency settings. Furthermore, correlating the clinical context with DECT's ability to discriminate between blood and calcium could decrease unnecessary admissions and reduce the costs of hospitalizing negative-ICH patients. The authors recommend using non-contrast brain DECT scans, especially in emergency settings.

What is already known on this topic?

Non-contrast CT scan has been used to detect intracerebral hemorrhage in head injury patients.

What does this study add?

Dual energy CT scan can improve detection of ICH by using blood (calcium subtraction) overlay image without an increased risk of radiation dose.

Acknowledgment

The authors gratefully acknowledge the contributions of Assist. Prof. Chulaluk Komoltri and Ms. Nerisa Thornsri who performed the statistical analyses for this research. The authors are also indebted to Mr. David Park for English-language editing.

Conflicts of interest

The authors declare that they have no potential conflicts of interest related to the research and did not receive any financial support for the research, authorship, or publication of this article.

References

1. Peterson AB, Xu L, Daugherty J, Breiding MJ. Surveillance report of traumatic brain injury-related emergency department visits, hospitalizations, and deaths, United States, 2014 [Internet]. 2019 [cited Apr 28]. Available from: https://stacks.cdc.gov/view/cdc/78062.
2. Bureau of Epidemiology, Department of Disease Control. Thailand's report situation of severe injuries year 2005-2010. Bangkok: Aksorn Grphic and Design Publishing; 2013.
3. Parizel PM, Makkat S, Van Miert E, Van Goethem JW, van den Hauwe L, De Schepper AM. Intracranial hemorrhage: principles of CT and MRI interpretation. Eur Radiol 2001;11:1770-83.
4. Aygun N, Masaryk TJ. Diagnostic imaging for intracerebral hemorrhage. Neurosurg Clin N Am 2002;13:313-34.
5. Bahner ML, Reith W, Zuna I, Engenhart-Cabillic R, van Kaick G. Spiral CT vs incremental CT: is spiral CT superior in imaging of the brain? Eur Radiol 1998;8:416-20.
6. Günther M. Perfusion imaging. J Magn Reson Imaging 2014;40:269-79.
7. Nute JL, Le Roux L, Chandler AG, Baladandayuthapani V, Schellingerhout D, Cody DD. Differentiation of low-attenuation intracranial hemorrhage and calcification using dual-energy computed tomography in a phantom system. Invest Radiol 2015;50:9-16.
8. Patino M, Prochowski A, Agrawal MD, Simeone FJ, Gupta R, Hahn PF, et al. Material separation using dual-energy CT: Current and emerging applications. Radiographics 2016;36:1087-105.
9. Henzler T, Fink C, Schoenberg SO, Schoepf UJ. Dual-energy CT: radiation dose aspects. AJR Am J Roentgenol 2012;199(5 Suppl):S16-25.
10. Yang NC, Leichner PK, Hawkins WG. Effective atomic numbers for low-energy total photon interactions in human tissues. Med Phys 1987;14:759-66.
11. Pomerantz SR, Kamalian S, Zhang D, Gupta R, Rapalino O, Sahani DV, et al. Virtual monochromatic reconstruction of dual-energy unenhanced head CT at 65-75 keV maximizes image quality compared with conventional polychromatic CT. Radiology 2013;266:318-25.
12. Nute JL, Jacobsen MC, Chandler A, Cody DD, Schellingerhout D. Dual-energy computed tomography for the characterization of intracranial hemorrhage and calcification: A systematic approach in a phantom system. Invest Radiol 2017;52:30-41.
13. Gupta R, Phan CM, Leidecker C, Brady TJ, Hirsch JA, Nogueira RG, et al. Evaluation of dual-energy CT for differentiating intracerebral hemorrhage from iodinated contrast material staining. Radiology 2010;257:205-11.
14. Wiggins WF, Potter CA, Sodickson AD. Dual-energy CT to differentiate small foci of intracranial hemorrhage from calcium. Radiology 2020;294:129-38.
15. Christner JA, Kofler JM, McCollough CH. Estimating effective dose for CT using dose-length product compared with using organ doses: consequences of adopting International Commission on Radiological Protection publication 103 or dual-energy scanning. AJR Am J Roentgenol 2010;194:881-9.
16. Almeida IP, Schyns LE, Öllers MC, van Elmpt W,

Parodi K, Landry G, et al. Dual-energy CT quantitative imaging: a comparison study between twin-beam and dual-source CT scanners. Med Phys 2017;44:171-9.

17. Coakley FV, Gould R, Yeh BM, Arenson RL. CT radiation dose: what can you do right now in your practice? AJR Am J Roentgenol 2011;196:619-25.